Rare Metal Materials and Engineering
Volume 54, Issue 10, October 2025
Available online at www.rmme.ac.cn

Science Press

Cite this article as: Wei Zhenwei, Tan Dongcan, Ma Li, et al. Influence of Overtemperature Treatment on Microstructure and Properties of Precision-Cast Ti_2AlNb Alloy[J]. Rare Metal Materials and Engineering, 2025, 54(10): 2453-2460. DOI: https://doi.org/10.12442/j.issn.1002-185X.20250027.

ARTICLE

Influence of Overtemperature Treatment on Microstructure and Properties of Precision-Cast Ti_2AlNb Alloy

Wei Zhenwei[1,5,6,7], Tan Dongcan[2], Ma Li[1,3,5,6,7], Zhou Qi[1,5,6,7], Zhao Jin[4], Liu Changkui[1,5,6,7]

[1] AECC Beijing Institute of Aeronautical Materials, Beijing 100095, China; [2] Nanchang Hangkong University, Nanchang 330063, China; [3] State Key Laboratory of Special Surface Protection Materials and Application Technology, Wuhan 430033, China; [4] Institute of Analysis and Testing, Beijing Academy of Science and Technology (Beijing Center for Physical & Chemical Analysis), Beijing 100089, China; [5] Failure Analysis Center, Aviation Industry Corporation of China, Beijing 100095, China; [6] Key Laboratory of Aeronautical Materials Testing and Evaluation, AECC, Beijing 100095, China; [7] Beijing Key Laboratory of Aeronautical Materials Testing and Evaluation, Beijing 100095, China

Abstract: Microstructure evolution of precision-cast Ti_2AlNb alloys after overtemperature treatments at 750 and 850 °C was investigated by optical microscope and scanning electron microscope, and Image J metallurgy analysis software was used for quantitative analysis. The variation of mechanical properties before and after overtemperature treatment was tested. Results show that the Ti_2AlNb alloy consists of B2 phase and lamellar O phase before and after overtemperature treatment. After overtemperature treatment, partial B2 phase is transformed into the O phase, and the lamellar structure of O phase suffers discontinuous coarsening and spherolization. The coarsening degree is increased with the increase in temperature and prolongation of treatment time, and O phase content is also gradually increased. The microhardness and tensile properties of Ti_2AlNb alloys at room and high temperatures are decreased with the increase in temperature and prolongation of treatment time, and the high-temperature tensile strength exhibits relatively larger decrement. An obvious linear relationship exists between microhardness and O phase content. Both the microhardness and the O phase content are important parameters to evaluate the overtemperature service damage degree of precision-cast Ti_2AlNb alloy.

Key words: Ti_2AlNb alloy; overtemperature; microstructure degradation; microhardness; tensile properties

1 Introduction

Ti_2AlNb alloys are novel TiAl-based intermetallic compounds, which are developed by adding element Nb into Ti_3Al intermetallic compounds[1]. Ti_2AlNb alloys exhibit excellent high-temperature yield strength, fracture toughness, creep resistance, low coefficient of expansion, and fine flame-retardant properties[2–4]. Compared with TiAl alloys, Ti_2AlNb alloys have better room-temperature ductility, fracture toughness, and crack resistance, and they have better high-temperature strength and oxidation resistance than Ti_3Al alloys. In addition, the density of Ti_2AlNb alloys is reduced by approximately 40% compared with that of iron- and nickel-based superalloys, but the high-temperature performance is basically unaffected[5]. The service temperature of Ti_2AlNb alloys is 200 °C, which is higher than that of titanium alloys. Due to these advantages, Ti_2AlNb alloys have great potential for application in the aerospace field, especially for the hot components of advanced aero-engines.

Aero-engine hot components have been serving under high-temperature, high-pressure gas, and complex stress conditions for a long time. The hot components are subjected to temperature and stress which change significantly under different operating conditions, such as the flame backwardness caused by insufficient fuel combustion, increased load, low oil pressure at the burner nozzle, inferior atomization of oil, and other abnormal engine conditions, leading to overtemperature service of the components, rapid decline of performance[6], and even disastrous accident[7]. The evolution of overheated microstructures and property degradation of wrought superalloy GH4033[8], as-cast equiaxial-crystal superalloy K465[9], directionally solidified

Received date: January 14, 2025
Corresponding author: Wei Zhenwei, Ph. D., Senior Engineer, AECC Beijing Institute of Aeronautical Materials, Beijing 100095, P. R. China, E-mail: 19801120205@163.com

superalloy[10], and single-crystal superalloy[11–12] have been widely researched. The researches of Ti_2AlNb alloys, as the alternatives to nickel-based superalloys, mainly focus on the control of the heat treatment[3,13–15], oxidation in high-temperature service[16], thermal corrosion[17–18], creep behavior[19], fracture mechanism[20], and service stability[21]. It is demonstrated that when the deformed Ti_2AlNb alloys are subjected to prolonged exposure at service temperatures, the α_2 lamellae undergo decomposition into fine O+B2 mixtures, and the incipient O phase is coarsened. This phenomenon results in a notable decline in the mechanical properties of Ti_2AlNb alloys[22]. Similarly, Ti-14Cu alloys exhibited static roughening behavior under prolonged thermal exposure, resulting in a reduction in plasticity[23]. Nevertheless, the microstructure and properties of Ti_2AlNb alloys under the overtemperature service conditions are rarely reported.

In this research, the precision-cast Ti_2AlNb alloy was selected as the research object. The microstructure evolution of the alloy after overtemperature treatment was characterized. The microhardness measurements and tensile tests at room temperature and 650 °C (high temperature) were conducted. The microstructure evolution, mechanical property degradation, and relationship between microstructure and property were obtained. This research provided the overtemperature service damage mechanism and established the evaluation method for the subsequent application on the aero-engine.

2 Experiment

In this research, all Ti_2AlNb alloy bars were firstly subjected to a standard heat treatment by hot isostatic pressing (1050 °C/160 MPa/4 h)+annealing treatment (980 °C/40 min). To avoid the effect of microstructure instability caused by batch differences, all experiment samples were taken from the same batch with the size specification of Φ15 mm×100 mm. The chemical composition of Ti_2AlNb alloy is shown in Table 1.

The long-term service temperature of the precision-cast Ti_2AlNb alloy was 650 °C. To align with the service conditions of Ti_2AlNb alloy, the thermal exposure treatment was conducted at 750 and 850 °C for 10 min – 2 h. The microhardness was tested using an MH-5L microhardness tester with a load of 0.5 kg and a holding time of 15 s. To ensure statistical reliability and minimize measurement variability, the final microhardness was determined by averaging 7 independent measurement results. To further verify the degradation of properties, three samples after thermal exposure for 0 min and 1 h were selected to perform the room- and high-temperature tensile tests. The tensile tests were conducted on an Instron-20 electronic universal testing machine with tensile rate of 1×10^{-4} s^{-1}. The loading method was axial loading. The room- and high-temperature tensile test methods are based on GB/T 228.1-2021 and GB/T 228.2-2015 standards, respectively. The sample dimensions are shown in Fig. 1. To ensure accuracy, three samples were prepared under each experiment condition, and the experiment data were averaged for analysis.

Table 1 Chemical composition of Ti_2AlNb alloy (wt%)

Al	Nb	C	Fe	H	N	O	Si	Y	Ti
10.44	41.70	0.006	＜0.10	0.0006	0.007	0.069	0.01	0.005	Bal.

Samples were progressively ground using 180#–2000# SiC abrasive paper, mechanically polished with an Alph-351 automatic grinder-polisher, and chemically etched in the specific solution ($HF:H_2O_2:H_2O$=1:6:3, vol%) at room temperature for 10 s. The morphology observation was conducted using an optical microscope, and the measurement of grain size was conducted by the truncation method. The microstructure was analyzed by scanning electron microscope (SEM, Zeiss GeminiSEM300) in secondary electron (SE) mode and backscattered electron (BSE) mode, and Image J software was used to measure the content of O and B2 phases with at least 5 SEM images. The specific quantitative method was reported in Ref.[24].

3 Results and Discussion

3.1 Microstructure analysis

Fig. 2 shows the grain morphology and microstructure of Ti_2AlNb alloy without overtemperature treatment. As shown in Fig.2a, the alloy consists of coarse grains with size of 2.19± 0.86 mm. Fig.2b shows SEM-BSE image of microstructure of Ti_2AlNb alloy. It can be seen that Ti_2AlNb alloy exhibits an obvious lamellar morphology, which consists of a bright-colored matrix and a black-grey lamellar phase. The chemical

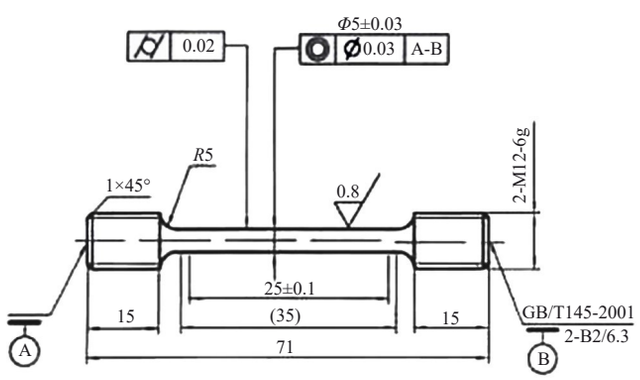

Fig.1 Schematic diagram of dimensions of tensile sample

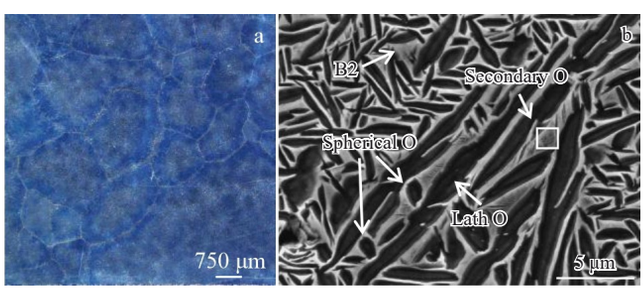

Fig.2 Grain morphology (a) and SEM-BSE microstructure (b) of Ti_2AlNb alloy without overtemperature treatment

composition of the O phase is Ti_2AlNb with an ordered orthorhombic crystal structure and the O phase serves as the Ti_2AlNb-based reinforcement phase within the alloy[25]. The B2 phase is characterized by a body-centered cubic structure and a space group. $Pm\bar{3}m$ is classified as a CsCl-type structure, which has a considerable number of vacancies, leading to a highly variable composition of B2 phase[26]. The discrepancies between different phases can be observed in BSE mode. The bright microstructure is B2 phase, and the dark grey lamellar microstructure is O phase. α_2 phase cannot be observed, and a small amount of secondary O phase is precipitated in the B2 phase, which is also reported in Ref.[27].

3.2 Microstructure evolution after overtemperature treatment

Fig. 3a and 3b show the grain morphologies of Ti_2AlNb alloy after different overtemperature treatments. It can be seen that there is no significant change in the grain size of Ti_2AlNb alloy after overtemperature treatment, compared with that before overtemperature treatment. The grain size is 1.98± 0.44 mm after overtemperature treatment at 850 °C for 2 h. Fig. 4 shows the microstructures of Ti_2AlNb alloy after different overtemperature treatments. It is found that the lamellar O phase is gradually coarsened, the number of spherical O phases decreases, and a small number of secondary O phases are gradually precipitated in the B2 phase with the prolongation of the overtemperature duration. In addition, the volume fraction of the B2 phase is decreased and the volume fraction of the O phase is increased gradually because of the B2→O phase transformation. The volume fraction of O phase in the Ti_2AlNb alloy is the highest when the overtemperature treatment condition is 850 °C/2 h. The changes in regularity of microstructure after overtemperature treatment at different temperatures are consistent, whereas the O phase of Ti_2AlNb alloy overheated at 850 °C is coarsened more seriously even under the same overtemperature time condition.

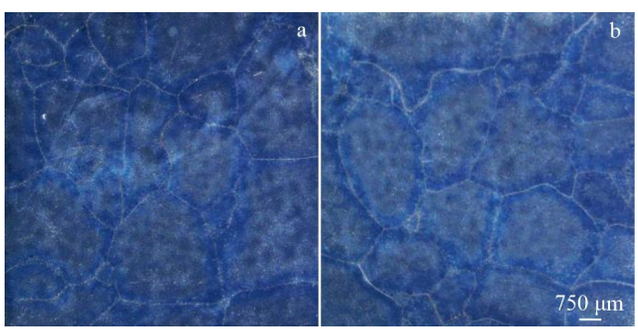

Fig. 3 Grain morphologies of Ti_2AlNb alloy after different overtemperature treatments: (a) 750 °C/20 min; (b) 850 °C/2 h

Quantitative analysis of the microstructure after overtemperature treatment was conducted by Image J software, and the result is shown in Fig. 5. With the increase in temperature and prolongation of treatment time, the O phase content of the Ti_2AlNb alloys is increased continuously, and the B2 phase content is decreased. This result indicates that the increase in temperature can accelerate the transformation from B2 phase to O phase. The O phase content increases from 57.40vol% to 71.70vol% and 76.30vol% after overtemperature treatment at 750 and 850 °C, respectively. The fitting curves of O phase content versus treatment time are also shown in Fig. 5. The data are fitted by polynomial y=Intercept+B_1x+B_2x^2, and the detail parameters of fitting curves are listed in Table 2. Thus, the relationship of O phase content of Ti_2AlNb alloy overheated at 750 and 850 °C with overtemperature time are simply expressed by Eq.(1–2), respectively:

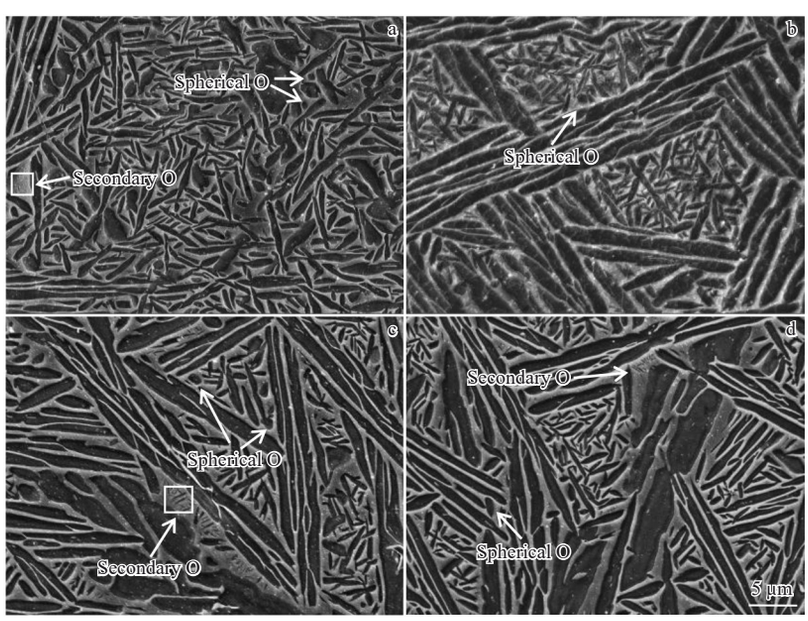

Fig.4 Microstructures of Ti_2AlNb alloy after different overtemperature treatments: (a) 750 °C/20 min; (b) 750 °C/2 h; (c) 850 °C/20 min; (d) 850 °C/2 h

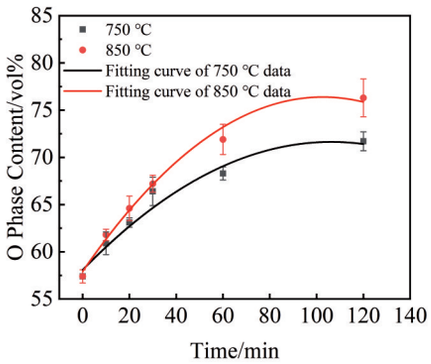

Fig.5 Volume fraction of O phase in alloys after overtemperature test and fitted curves

$$V = 58.08 + 0.26t - 0.0012t^2 \quad (R^2=0.96) \tag{1}$$

$$V = 57.92 + 0.36t - 0.0018t^2 \quad (R^2=0.98) \tag{2}$$

where V is the volume fraction of O phase and t is the overtemperature time (min).

The transformation from B2 phase into O phase proceeds through the diffusion process, and the increasing rate of O phase content becomes slower with the prolongation of the treatment time, which may be due to the energy depletion in the initial stage, leading to the energy shortage in the later stage[28] and then the decrease in transformation rate. The relationship between diffusion coefficient (D) and temperature[29] is expressed by Eq.(3), as follows:

$$D = D_0 \exp(-Q/RT) \tag{3}$$

where D_0 is pre-exponential factor, Q is the diffusion activation energy, R is gas constant, and T is thermodynamic temperature. According to Eq. (3), the temperature-dependent enhancement in diffusion coefficient is accompanied with accelerated transformation kinetics from the B2 to O phase.

The Ostwald mechanism controls the initial stage of O phase coarsening at high temperatures. This phenomenon can be explained by the fact that the Gibbs free energy of large-sized O phase grains is lower than that of small-sized grains. The difference in energy provides a driving force for the fusion of O phase grains of different sizes[30], which results in the decrease in the number of spherical O phases with the aggravation of O phase coarsening. Lifshitz-Slyozov-Wagner (LSW) theory was developed based on this theory[31], as follows:

$$\bar{r}^3(t) - \bar{r}_0^3(t=0) = Kt \tag{4}$$

where $\bar{r}(t)$ is the mean radius of the precipitates, $\bar{r}_0(t=0)$ is the initial mean radius of the precipitates, K is coarsening rate constant, and t is heat treatment time. Consistent with LSW theory, prolonged overtemperature time promotes O phase coarsening kinetics, demonstrating good agreement with microstructure observation. This classical theory is based on the assumption that the volume fraction of precipitates is infinitesimal and the spherical precipitation phase is almost fully coherent with the matrix[32]. Therefore, the classical LSW theory should be modified[33], as follows:

$$d = Kt^n \tag{5}$$

where d is the average size of lamellae, K is coarsening rate constant, t is the heat treatment time, and n is coarsening coefficient. The modified theory can be applied to a two-phase titanium alloy.

O phase coarsening is governed by a termination migration mechanism during prolonged overtemperature treatment. Due to different interfacial energies of the lamellar O phase along terminal and long-axis directions, the diffusion behavior is different, the lamellar O phase undergoes static spheroidization, and the spheroid O phase grows again into the coarser lamellar O phase by Ostwald coarsening[34]. These phenomena all account for the slow increase of O phase content at the late overtemperature stage. This coarsening mechanism is also reported in Ref.[34–35].

3.3 Degradation analysis

Fig. 6a shows the microhardness of Ti_2AlNb alloy after different overtemperature treatments. It can be seen that the microhardness is decreased with the prolongation of treatment time, and it decreases rapidly in the first 30 min. The microhardness exhibits an inverse correlation with overtemperature levels under the equivalent treatment time. The microhardness of Ti_2AlNb alloy before overtemperature treatment is 322 HV, and it decreases to 292 and 285 HV after overtemperature treatments of 750 °C/2 h and 850 °C/2 h, which decreases by 9.32% and 11.49%, respectively. The microhardness is decreased with the prolongation of treatment time, whose variation trend is opposite to that of O phase content, but the variation rate of both parameters decreases. The change in microhardness can be used to characterize the degree of damage of Ti_2AlNb alloys in the overtemperature service.

The microhardness is linearly fitted to the O phase content, and the results are shown in Fig. 6b and Table 3. Thus, the linear relationship is simplified, as follows:

$$Y_{\text{microhardness}} = 423.91 - 1.85V_{\text{total}} \tag{6}$$

where V_{total} is the volume fraction of O phase and $Y_{\text{microhardness}}$ is microhardness. The fitting results only consider the correlation between O phase content and microhardness, which is derived through the combination of O phase quantification and microhardness measurements after overtemperature treatments at two distinct thermal conditions.

Table 2 Parameters of fitting curves of O phase content in Fig.5

Temperature/°C	Intercept	Standard error of intercept	B_1	Standard error of B_1	B_2	Standard error of B_2/×10^{-4}	R^2
750	58.08	0.69	0.26	0.035	−0.0012	2.92	0.96
850	57.92	0.45	0.36	0.032	−0.0018	2.92	0.98

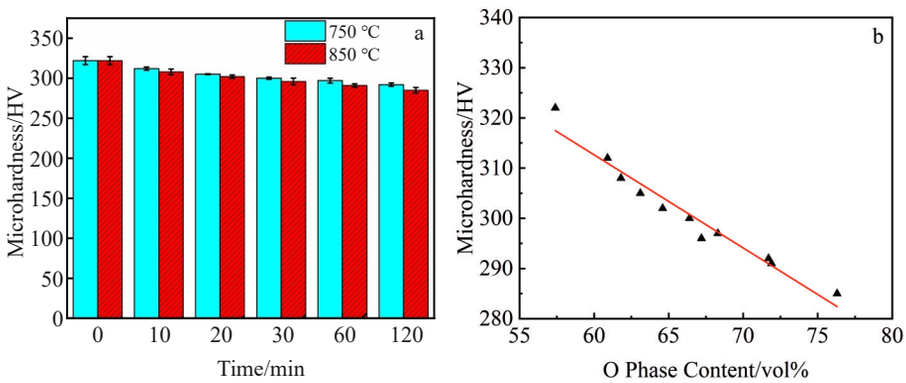

Fig.6 Microhardness of Ti_2AlNb alloy after different overtemperature treatments (a); relationship between microhardness and O phase content of Ti_2AlNb alloy (b)

The regression analysis reveals that the variation in microhardness exhibits a linear dependence on the content change with R^2 of approximately 0.95, demonstrating statistically robust agreement between the experiment data and theoretical prediction.

The microhardness of Ti_2AlNb alloys exhibits an inverse correlation with lamellar O phase width[34], i.e., the coarser the lamellar microstructure, the less the microhardness. However, the Ti_2AlNb alloy used in this research consists of only lamellar O and B2 phases, and the increase in O phase content is mainly caused by the coarsening of lamellar O phase.

Fig. 7 shows the variation trend of the room-temperature tensile properties of Ti_2AlNb alloy after different overtemperature treatments. According to Fig.7a, it can be concluded that the ultimate tensile strength after overtemperature treatment shows a decreasing trend with the prolongation of treatment time, and ultimate tensile strength at room temperature demonstrates a temperature-dependent degradation. Under the same treatment time, the higher the temperature, the larger the strength decrement. The ultimate tensile strength of Ti_2AlNb alloy decreases from 956 MPa to 880 and 850 MPa after overtemperature treatments of 750 °C/1 h and 850 °C/1 h, which decreases by 7.94% and 14%, respectively. This result indicates that both the time and temperature of overtemperature treatment affect the ultimate tensile strength of Ti_2AlNb alloy at room temperature. The elongation of the Ti_2AlNb alloy also shows a decreasing trend with the prolongation of treatment time, as shown in Fig. 7b. Elongation performance exhibits a pronounced inverse correlation with overtemperature levels under equivalent treatment time. The elongation decreases from the initial 10.90% to 5.30% and 4.10% after overtemperature treatments of 750 °C/1 h and 850 °C/1 h, respectively. The deterioration in plasticity of Ti_2AlNb alloy after overtemperature treatment is related to the coarsening of O phase in Ti_2AlNb alloy. The variation trends of ultimate tensile strength and elongation at room temperature are in agreement with that of microhardness. Therefore, for Ti_2AlNb alloy after overtemperature treatment, the microhardness variation can reflect the variation of room-temperature tensile properties.

Table 3 Parameters of fitting line $y=a+bx$ in Fig.6b

a	Standard error of a	b	Standard error of b	R^2
423.91	9.02	−1.85	0.14	0.95

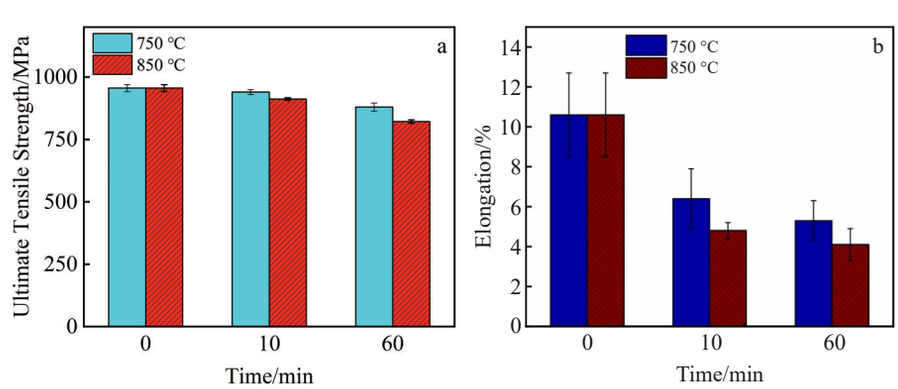

Fig.7 Effects of overtemperature treatments on ultimate tensile strength (a) and elongation (b) of Ti_2AlNb alloy at room temperature

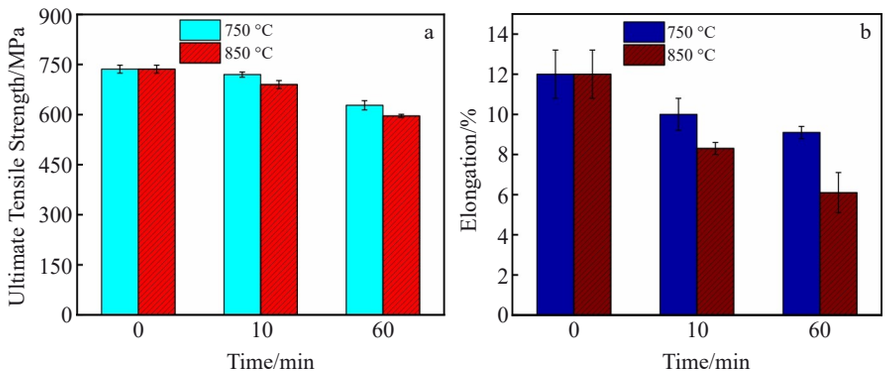

Fig.8 Effects of overtemperature treatments on ultimate tensile strength (a) and elongation (b) of Ti_2AlNb alloy at 650 °C

Fig. 8 shows the variation trend of the high-temperature (650 ° C) tensile properties of Ti_2AlNb alloy after different overtemperature treatments. It can be seen that the changes in tensile properties of Ti_2AlNb alloy at high temperature are similar to those at room temperature. The tensile properties are degraded with the increase in temperature and the prolongation of treatment time, which indicates that overtemperature treatment produces irreversible mechanical property damage to Ti_2AlNb alloy. The high-temperature ultimate tensile strength of the Ti_2AlNb alloy decreases from 740 MPa to 628 and 601 MPa after overtemperature treatments of 750 °C/1 h and 850 °C/1 h, which decreases by 15.14% and 18.78%, respectively. The decrement in high-temperature ultimate tensile strength is larger than that of room-temperature ultimate tensile strength. The elongation decreases from 12.00% to 9.10% and 6.10% after overtemperature treatments of 750 ° C/1 h and 850 ° C/1 h, respectively. The high-temperature elongation is comparable to the room-temperature elongation. The variation trend of the high-temperature tensile properties is also consistent with that of the microhardness, indicating that the microhardness variation can also reflect the variation of high-temperature tensile properties of Ti_2AlNb alloy after overtemperature treatment.

The microhardness, tensile strength, and elongation of Ti_2AlNb alloys are gradually decreased with microstructure changes, which bring irreversible overtemperature service damage. The main microstructure parameters affecting the tensile strength of Ti_2AlNb alloys include grain size, phase size and content, and secondary O phase of the alloy. For grain size, the tensile strength of Ti_2AlNb alloys follows the Hall-Petch relationship, and the mechanical properties of the alloys are improved with the decrease in grain size[36]. However, in this research, the grain size of the overtemperature-treated Ti_2AlNb alloy is unchanged, so the effect of grain size on the mechanical properties of the alloy is excluded.

Chen et al[28] demonstrated that the thickness of lamellar O phase in Ti_2AlNb alloys follows the Hall-Petch strengthening relationship, and the coarsening of O phase reduces the yield strength but enhances ductility. However, fine secondary O phase precipitates form during overtemperature treatment, improving the strength and diminishing the plasticity. At the same time, the content of B2 phase continuously decreases with the coarsening of lamellar O phase and the precipitation of secondary O phase, which is a plastic phase with a large number of slip systems, and the decrease in B2 phase content leads to a decrease in the plasticity of the alloy[27,37–38]. The spherical O phase is also considered to improve plasticity. Slip can be more easily transferred through the grain boundaries of the O/B2 phase, and the combination of the spherical O phase and the B2 phase contributes to better strength and plasticity[39]. After overtemperature treatment, the Ti_2AlNb alloy exhibits the coarsening of lamellar O phase with the decrease in spherical O phase content and the precipitation of secondary O phase. Both room-temperature and high-temperature ultimate tensile strength are greatly reduced due to the coarsening of lamellar phase and the decrease in spherical phase, which also results in the degradation of microhardness. The improvement in plasticity caused by the coarsening of the lamellar O phase is insufficient to offset the reduction in ductility caused by the decrease in the content of B2 phase and spherical O phase. The limited secondary O phase content indicates that the reduction in the content of B2 phase and spherical O phase mainly decreases the plasticity.

Nevertheless, the aero-engine components in practice are subjected to numerous factors, including high temperatures, high pressures, and corrosive substances. Therefore, it is necessary to simulate a more realistic operating environment and consider more environmental factors to assess the impact of service damage.

4 Conclusions

1) After overtemperature treatment of Ti_2AlNb alloy, the B2 phase is transformed into the O phase, and the lamellar O coarsens. In the initial stage, the coarsening of lamellar O phase is controlled by the Ostwald mechanism. With the prolongation of the treatment time, the coarsening of O phase is controlled by the terminal migration mechanism. The O phase content increases from 57.40vol% to 71.70vol% and 76.30vol% after overtemperature treatment of 750 °C/2 h and

850 °C/2 h, respectively.

2) The microhardness of the overtemperature-treated Ti_2AlNb alloy exhibits a decreasing variation. The microhardness decreases by 9.32% after overtemperature treatment at 750 °C for 2 h, and it decreases by 11.49% after overtemperature treatment at 850 °C for 2 h. The O phase content exhibits a significant linear correlation with microhardness when isolated from other microstructural variables:

$$Y_{\text{microhardness}} = 423.91 - 1.85V_{\text{total}}$$

The R^2 value of this linear fitting is 0.948 97, demonstrating excellent correlation.

3) After overtemperature treatment, the Ti_2AlNb alloy exhibits decreasing trends in both ultimate tensile strength and elongation at room temperature and high temperature (650 °C). High-temperature strength demonstrates greater sensitivity to O phase coarsening and content variations compared with that at room temperature. The variation trend of microhardness aligns with that of tensile properties. The degradation extent caused by overtemperature can be effectively assessed through microhardness measurements or O phase content analysis.

References

1 Dai J, Sun C, Wang A *et al*. *Corros Sci*[J], 2021, 184: 109336

2 Yin Xuchen, Chen Zhiyong, Wang Qingjiang *et al*. *Rare Metal Materials and Engineering*[J], 2024, 53(8): 2293 (in Chinese)

3 Hong Y Z, Chong L, Zong Q M *et al*. *Int J Min Met Mater*[J], 2018, 25(10): 1191

4 Wei Z W, Ma L, You L *et al*. *J Phy: Conference Series*[J], 2024, 2686: 012024

5 Zhang H Y, Yan N, Liang H Y *et al*. *J Mater Sci Technol*[J], 2021, 80: 203

6 Bu J L, Gao Z K, Han Z Y *et al*. *Failure Analysis and Prevention*[J], 2020, 15(3): 179

7 Zhao Yunsong, Zhang Mai, Guo Xiaotong *et al*. *J Mater Eng*[J], 2020, 48(9): 24 (in Chinese)

8 Tong Jinyan, Feng Wei, Fu Chao *et al*. *Acta Metall Sin*[J], 2015, 51(10): 1242 (in Chinese)

9 Guo Xiaotong, Zheng Weiwei, Xiao Chengbo *et al*. *J Mater Eng*[J], 2018, 46(10): 77 (in Chinese)

10 An W R, Zheng W W, Zheng Y R *et al*. *J Rare Met*[J], 2020, 44(10): 1009

11 Yang Y Z, Wen Z X, Pei H Q *et al*. *Progress in Nature Science: Materials International*[J], 2023, 33(3): 33

12 Peng S, Shi F X, Teng Y F *et al*. *Failure Analysis and Prevention*[J], 2024, 19(2): 99

13 Zhao Hongze, Lu Bing, Yang Rui. *J Nonferrous Met*[J], 2017, 27(4): 708 (in Chinese)

14 Huang Dong, Wei Zhanlei, Zhu Langping *et al*. *Special Casting & Nonferous Alloys*[J], 2018, 38(8): 835 (in Chinese)

15 Bu Z Q, Zhang Y G, Yang L *et al*. *Journal of Alloys and Compounds*[J], 2022, 893: 162364

16 Dadé M, Esin V A, Nazé L *et al*. *Corros Sci*[J], 2019, 148: 379

17 Yong S H, Rui H, Wen Z L *et al*. *Rare Metals*[J], 2018, 37(10): 838

18 Deng Z Z, Dai Z F, Wu W B *et al*. *Rare Metal Materials and Engineering*[J], 2024, 53(10): 2755

19 Yang S J, Nam S W, Hagiwara M. *Intermetallics*[J], 2004, 12(3): 261

20 Tang W, Shao B, Zong Y Y *et al*. *J Mater Res Technol*[J], 2022, 20: 1291

21 Zhang T B, Huang G, Hu R *et al*. *T Nonferr Metal Soc*[J], 2015, 25(8): 2549

22 Shang Z, Niu H J, Wang A *et al*. *Journal of Materials Research and Technology*[J] 2024, 30: 1095

23 Jiang C P, Zhang L X, Chen Y N *et al*. *Journal of Alloys and Compounds*[J], 2021, 882: 160685

24 Wang Kaixuan, Zeng Weidong, Shao Yitao *et al*. *Rare Metal Materials and Engineering*[J], 2009, 38(3): 398 (in Chinese)

25 Li Ping, Ding Ruidong, Zhang Yongqiang *et al*. *Rare Metal Materials and Engineering*[J], 2024, 53(6): 1701 (in Chinese)

26 Chen Y Y, Yue H Y, Wang X P *et al*. *Materials Characterization*[J], 2018, 142: 584

27 Li N, Zhao Z B, Sun H *et al*. *Mat Sci Eng A*[J], 2022, 857: 144052

28 Chen X, Wei D Z, Wei W *et al*. *Mat Sci Eng A*[J], 2014, 611: 320

29 Liu S Z, Shi Z X, Han M *et al*. *Materials Science Forum*[J], 2017, 898: 517

30 Zhang H Y, Li C, Ma Z Q *et al*. *Vacuum*[J], 2019, 169: 108934

31 Lifshitz I M, Slyozov V V. *J Phys Chem Solids*[J], 1961, 19(1–2): 35

32 Xu J W, Zeng W D, Sun X *et al*. *Journal of Alloys and Compounds*[J], 2015, 631: 248

33 Zherebtsov S, Murzinova M, Salishchev G *et al*. *Acta Mater*[J], 2011, 59(10): 4138

34 Zhou X, Liu J, Zhang S M *et al*. *J Mater Res Technol*[J], 2023, 27: 4236

35 Xue C, Zeng W D, Wang W *et al*. *Mat Sci Eng A*[J], 2013, 587: 54

36 Li S Q, Mao Y, Zhang J W *et al*. *T Nonferr Metal Soc*[J], 2002, 12(4): 582

37 Huang Y, Liu Y C, Zhang Y R *et al*. *Journal of Alloys and Compounds*[J], 2020, 842: 155794

38 Jiao X Y, Wang D J, Yang J L *et al*. *Journal of Alloys and Compounds*[J], 2019, 789: 639

39 Wang W, Zeng W D, Xue C *et al*. *Intermetallics*[J], 2015, 56: 79

超温处理对精密铸造Ti_2AlNb合金组织及性能的影响

魏振伟[1,5,6,7]，谭东灿[2]，马　力[1,3,5,6,7]，周　麒[1,5,6,7]，赵　瑾[4]，刘昌奎[1,5,6,7]

(1. 中国航发北京航空材料研究院，北京 100095)

(2. 南昌航空大学，江西 南昌 330063)

(3. 特种表面保护材料及应用技术国家重点实验室，湖北 武汉 430033)

(4. 北京市科学技术研究院 分析测试研究所(北京市理化分析测试中心)，北京 100089)

(5. 中国航空工业集团公司 失效分析中心，北京 100095)

(6. 中国航空发动机集团 材料检测与评价重点实验室，北京 100095)

(7. 航空材料检测与评价北京市重点实验室，北京 100095)

摘　要：采用光学显微镜、扫描电子显微镜研究了精密铸造Ti_2AlNb合金在750和850 ℃下超温处理后的组织演变，并使用Image J金相分析软件进行定量分析，同时测试了超温前后的力学性能变化。结果表明：Ti_2AlNb合金超温前后均由B2相和O相板条组成；超温处理后，部分B2相转变为O相，且O相板条组织发生不连续粗化和球化，粗化程度随着超温温度的增加和超温时间的延长而加重，O相含量也逐渐增加；Ti_2AlNb合金的显微硬度与室温、高温拉伸性能均随着超温温度的增加和超温时间的延长而下降，且高温抗拉伸强度下降幅度更大；显微硬度与O相含量间存在显著线性关联，O相含量及显微硬度均是表征Ti_2AlNb合金超温服役损伤程度的关键参量。

关键词：Ti_2AlNb合金；超温；组织退化；显微硬度；拉伸性能

作者简介：魏振伟，男，1986年生，博士，高级工程师，中国航发北京航空材料研究院，北京 100095，E-mail：19801120205@163.com